

2012

# Experimental Investigation of Temporary Electronics Cooling with Regularly Structured Composite Latent Heat Storages

Ekkehard Lohse  
Ekkehard.Lohse@tuhh.de

Gerhard Schmitz

Follow this and additional works at: <http://docs.lib.purdue.edu/iracc>

---

Lohse, Ekkehard and Schmitz, Gerhard, "Experimental Investigation of Temporary Electronics Cooling with Regularly Structured Composite Latent Heat Storages" (2012). *International Refrigeration and Air Conditioning Conference*. Paper 1219.  
<http://docs.lib.purdue.edu/iracc/1219>

This document has been made available through Purdue e-Pubs, a service of the Purdue University Libraries. Please contact [epubs@purdue.edu](mailto:epubs@purdue.edu) for additional information.

Complete proceedings may be acquired in print and on CD-ROM directly from the Ray W. Herrick Laboratories at <https://engineering.purdue.edu/Herrick/Events/orderlit.html>

## Experimental Investigation of Temporary Electronics Cooling with Regularly Structured Composite Latent Heat Storages

Ekkehard LOHSE<sup>1\*</sup>, Gerhard SCHMITZ<sup>2</sup>

Hamburg University of Technology, Institute of Thermo-Fluid Dynamics,  
Applied Thermodynamics, Hamburg, Germany  
<sup>1\*</sup>ekkehard.lohse@tu-harburg.de

Hamburg University of Technology, Institute of Thermo-Fluid Dynamics,  
Applied Thermodynamics, Hamburg, Germany  
<sup>2</sup>schmitz@tu-harburg.de

### ABSTRACT

This study shows results of the experimental investigation of regularly structured Composite Latent Heat Storages. Common solid-liquid Phase Change Materials used as latent heat storages have a low thermal conductivity, which leads to high temperature differences inside large PCM volumes. This drawback is compensated by the combination with specially designed frame-structures made of aluminum to enhance the transport of thermal energy inside the regularly structured Composite Latent Heat Storage.

A prototype is investigated experimentally on a test rig, where the heat load and temperatures are measured while the phase change process is observed optically. The results are compared to a solid block PCM heat storage.

Keywords: Latent heat storages, Phase Change Materials, Thermal conductivity.

### 1. INTRODUCTION

Latent heat storages are very reliable passive cooling systems. Due to their high latent heat of fusion, Phase Change Materials (PCM) can be used in light-weight heat storages (Dincer, 2002), e. g. for cooling applications in modern aircraft. Heat storages buffer waste heat peak loads and thus enable the designers to build smaller, lighter cooling systems or they provide back-up cooling functions in case of a failure in the active systems.

However the low thermal conductivity of common PCMs, e.g. paraffins or salt hydrates, is a challenge in the design of such cooling systems. State-of-the-art is the combination with a random supporting structure of metal or carbon foams to improve the distribution of thermal energy inside latent heat storages. With the new manufacturing method of Selective Laser Sintering (SLS) it is possible to design the supporting structure in order to optimize the transport of waste heat from specific heat sources into the PCM.

This paper gives an overview of the potential of regularly structured Composite Latent Heat Storages (CLHS) manufactured by SLS. Regularly structured CLHS prototypes are investigated experimentally at the Institute of Thermo-Fluid Dynamics and the results compared to plain solid block PCM heat storages.

### 2. COMPOSITE LATENT HEAT STORAGE

To improve the thermal conductivity of latent heat storages PCMs are combined with materials of high thermal conductivity. Frame structures made of aluminum are manufactured by SLS and filled with PCM resulting in regularly structured CLHS.

## 2.1 Thermodynamic Properties

The most commonly used PCMs are paraffins and salt hydrates, with paraffins having the higher specific latent heat of fusion while being lighter (Mehling, 2008). For electronics cooling there are many PCMs with fusion temperatures between ambient and  $T = 100$  °C. Typical values for the thermodynamic properties density  $\rho$ , specific heat capacity  $c$  and thermal conductivity  $k$  are given in table 1. It clearly shows the very low thermal conductivity ( $k < 1$  W/(mK)) and the thermal diffusivity  $\alpha$ . The table also gives the fusion temperature and the latent heat of fusion of the PCM *PARAFOL 22-95*<sup>®</sup>.

**Table 1:** Material properties of aluminum (COMSOL, 2011) and PCM *PARAFOL*<sup>®</sup> 22-95 (Sasol, 2010).

Property	Aluminum AlSi12	<i>PARAFOL</i> <sup>®</sup> 22-95
Density $\rho$ in kg/m <sup>3</sup>	2700	777
Specific heat capacity $c$ in J/kgK	900	3300
Thermal conductivity $k$ in W/mK	160	0,162
Thermal diffusivity $\alpha$ in 10 <sup>-6</sup> m <sup>2</sup> /s	65,84	0,063
Fusion temperature in °C	-	41.6
Latent heat of fusion in kJ/kg	-	250

*PARAFOL 22-95*<sup>®</sup> produced by *Sasol Olefins and Surfactants GmbH* is a pure paraffin which has a very high latent heat of fusion and comparably high specific heat capacity (Sasol, 2010). The fusion temperature of  $T_f = 41.6$  °C is not very high for electronics cooling but it is sufficient to show the concept of regularly structured CLHS. For a real application the PCM can be exchanged easily by one with a higher fusion temperature.

For comparison the thermodynamic properties of aluminum AlSi12 are given in table 1 as well. It is the material that is used in manufacturing of the frame-structures and has a high thermal conductivity, especially compared to *PARAFOL 22-95*<sup>®</sup>. Additionally to the thermal conductivity the thermal diffusivity takes the density and specific heat capacity into account and shows clearly the difference in transport of inner energy inside a material between the PCM and the aluminum.

## 2.2 Selective Laser Sintering

Selective laser sintering is an additive manufacturing technique. The schematic is shown in figure 1. Raw material in pulverized condition is used to generate the final product. It is stored in the powder reservoir and supplied to the fabrication bed in thin layers by a delivery system. Once a layer is applied, a laser-scanner system is used to fuse the powder at the positions specified in a 3-D CAD-model. After one layer is finished the fabrication bed is lowered and new powder is applied. The laser now fuses the powder again creating the layer's geometry and connecting it to the layer below.

The design of parts is only limited by material selection and the layer-wise generation, which requires a solid connection between all the layers. The layer thickness and the smallest diameter of the solid regions are determined by the laser focus of 60  $\mu$ m to 90  $\mu$ m resulting in melting region of about 200  $\mu$ m. The material used for heat storage frame-structures is the aluminum alloy AlSi12, which provides high thermal conductivity.

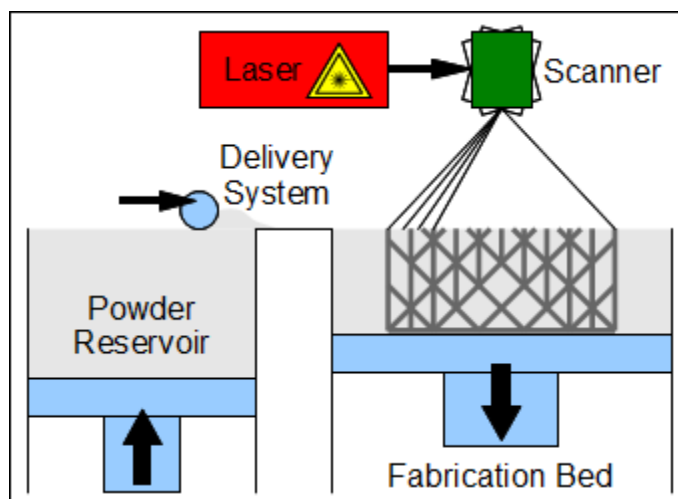


**Figure 1:** Selective Laser Sintering (SLS) schematic.

### 2.3 Regularly Structured Composite Latent Heat Storages

The combination of PCM for high heat storage capacity and aluminum for the distribution of thermal energy leads to CLHS. The advantage of regular structures in comparison to irregular foams is the possibility to design the thermally conductive frame-structure for special cooling applications, where the waste heat of components is not uniform but depends on the geometric position. Integrated electronic components often have Hot-Spots, regions in which high thermal loads have to be removed, and a customized regularly structured CLHS provides improved cooling performance.

However the basic regularly structured CLHS is a solution for homogeneous heat sources, which is investigated experimentally in this paper. The frame-structure used is a quadratic grid with 0.5 mm thick aluminum walls creating 225 PCM volumes (15x15). The PCM volumes have a cross-section of 3 mm x 3 mm and are 52 mm deep.

## 3. TEST RIG

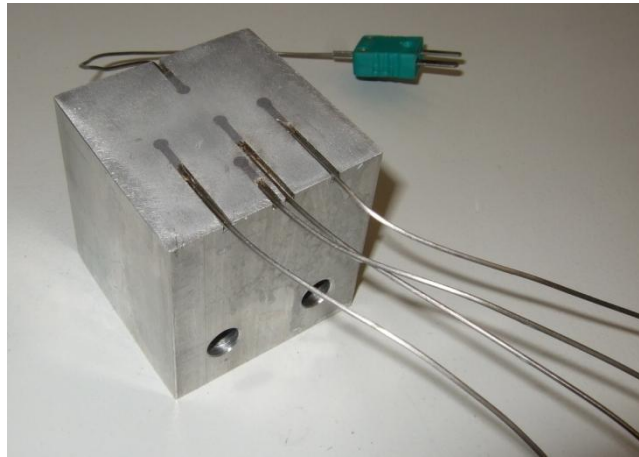
A test rig at the Institute of Thermo-Fluid Dynamics is used to investigate the performance of a basic regularly structured CLHS as electronics cooling system in comparison to a plain solid block PCM heat storage.

### 3.1 Set up

The main parts of the test rig are the latent heat storage and the heat source, which are sufficiently insulated to the ambient. The heat source, shown in figure 2, is a solid aluminum cube with a base length of 50 mm. Two holes are applied at the bottom to insert electric cartridge heaters that produce heat, which is distributed in the heat block. Five type K thermocouples are soldered on the top of the heat block to measure the temperatures at the heat transfer interface.

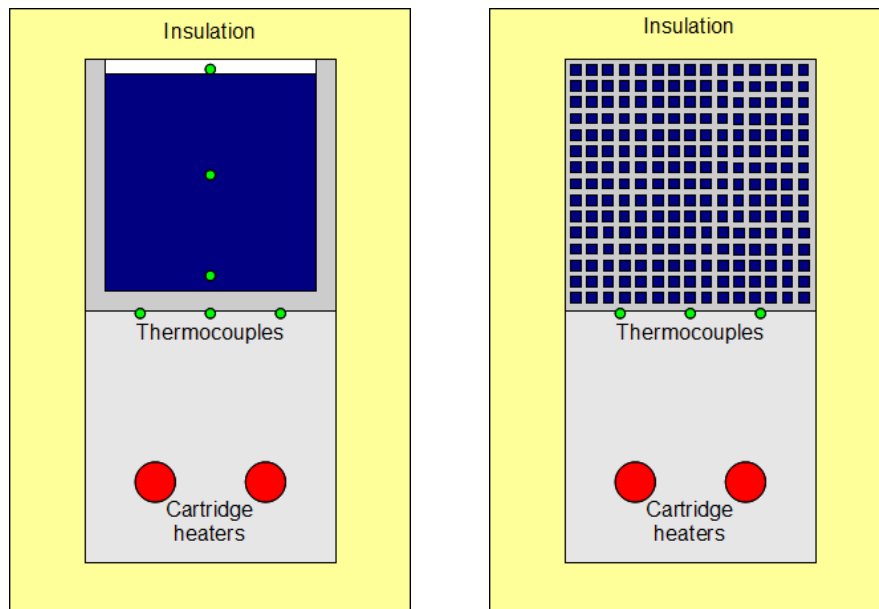
The heat storage is replaceable and mounted on top of the heat block. In this study two different heat storages are used. To improve the heat transfer between both solid surfaces a thermal interface material is applied.

Figure 3 (left) shows the set up for the reference plain solid block PCM heat storage. The PCM is filled into a U-shaped aluminum profile with a thickness of 4 mm and a base length of 50 mm. Two transparent walls create a cubic volume (resulting base length 42 mm) for the PCM inside the U-profile. The wall material is polycarbonate which has a similar thermal conductivity as the PCM and allows the optical observation of the phase change process. An air volume above the PCM compensates the density change from solid to liquid. From the open top of the heat storage optional thermocouples measure the temperatures inside the PCM and in the air above during the fusion process. However they change the fusion pattern due to their high thermal conductivity and are removed for direct comparison.



**Figure 2:** Heat block with holes for cartridge heaters and thermocouples soldered onto the heat transfer surface.

Figure 3 (right) shows the set up with regularly structured CLHS. The prototype is shown in figure 4. It has a transparent wall as well through which the PCM and the frame-structure are visible. In this heat storage no thermocouples are placed inside the PCM.



**Figure 3:** Test rig set up: heat block, heat storage and insulation; *left*: U-profile heat storage with optional thermocouples in the PCM; *right*: Regularly structured CLHS prototype with quadratic frame-structure.

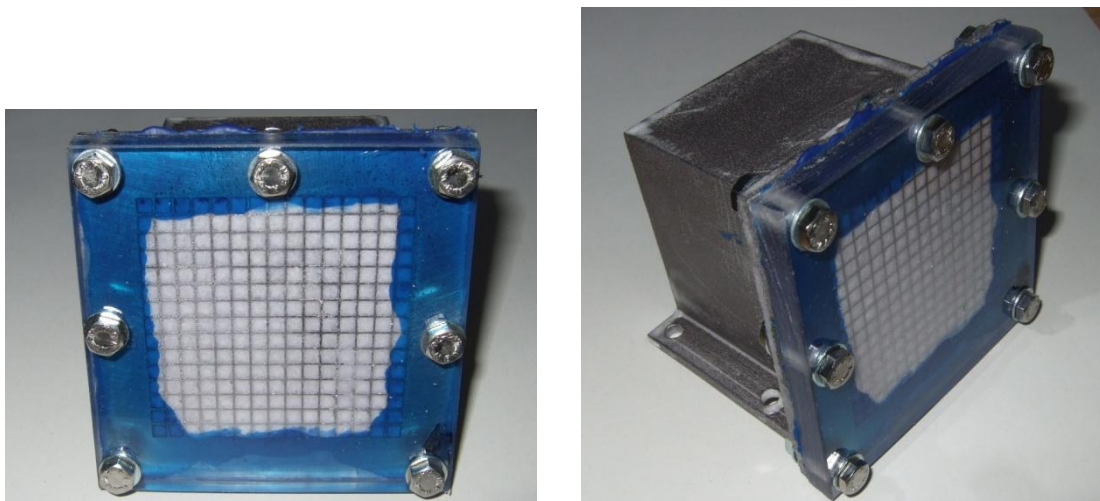


**Figure 4:** Frame-structure Quad: regularly structured CLHS prototype with transparent wall.

### 3.2 Measurement Equipment and Test Plan

A *National Instruments* data acquisition (DAQ) system is used to monitor the tests and save the measurement data with *LabVIEW*. The controller for the electric heating cartridges has an energy meter, which measures the voltage and current applied. The resulting heat load is transferred into a current signal of  $I = 4...20$  mA and logged by the DAQ system. The temperatures at the heat block are measured by type K thermocouples (accuracy:  $\pm 1.5$  K) while type T thermocouples (accuracy:  $\pm 0.5$  K) are used for the measurements inside the PCM. Cold junction compensation is integrated in the DAQ system. The camera used to observe the phase change process has a resolution of  $240 \times 320$  pixels. Every 10 s all measurement data as well as the pictures are stored.

At the beginning of a test the insulation is fixed around the test devices and the camera is adjusted and focused on the heat storage's transparent wall. Then a heat load is set at the controller. It is kept constant over the whole testing time. All data and the camera pictures are stored, while the heat block and storage temperatures rise. When the total PCM is liquid or when the measured temperatures reach  $T = 150$  °C the heat load is switched off. The regeneration of the heat storage is observed as well, however this process will not be discussed in this paper.

The maximum heat load for the electric cartridge heaters is  $\dot{Q} = 200$  W. However experiments with useable measurement data are conducted with smaller heat loads up to  $\dot{Q} = 100$  W. In this study three different heat loads  $\dot{Q}_{low} = 50$  W,  $\dot{Q}_{mid} = 75$  W and  $\dot{Q}_{high} = 100$  W are compared.

## 4. EXPERIMENTAL RESULTS

In this section the temperature measurements and the pictures during the fusion process are presented and discussed for the solid block PCM heat storage as a reference and the regularly structured CLHS prototype with quadratic frame-structure.

### 4.1 Solid block PCM heat storage

The five temperatures on the top of the heat source are almost equal, thus figure 5 shows only one temperature plot for each applied heat load. According to the test plan three different heat loads are applied with the electric cartridge heaters.

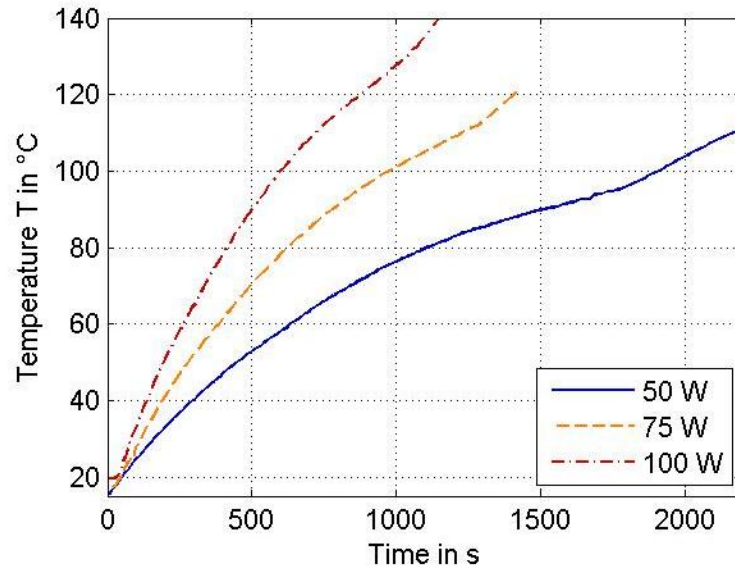


**Figure 5:** Thermal interface temperatures with U-profile for three different heat loads.

Not surprisingly the temperature rises faster for higher heat loads, however the behavior is not as it would be expected for a combination of sensible and latent heat storage. The fusion process in the PCM starts around  $T = 40$  °C PCM temperature. Considering the thermal interface between heat block and heat storage and the aluminum wall of the storage itself a gradient change due to latent heat storage is expected at temperatures above  $T = 40$  °C heat storage temperature. On the contrary the onset of fusion cannot be determined from the plots, as there is not significant change measured in the gradient. The reason for this observation is the low thermal conductivity of the PCM, as described in the introduction.

Nevertheless the experiments show the end of fusion with a gradient change in the temperature plots and are used to assess the thermal performance of the regularly structured CLHS prototype.

As described in the test rig set up a camera is used to observe the fusion process. Figure 6 shows four characteristic pictures during the fusion process. The aluminum U-profile is clearly visible as well as the screws used for assembly (Figure 6, left). The solid PCM is represented white while the liquid PCM gets transparent and is black in all pictures because of the black background.

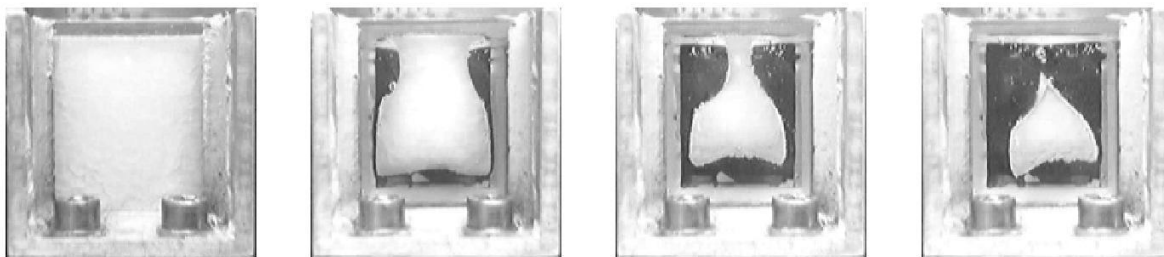


**Figure 6:** Phase change process in U-profile heat storage; *from left to right*: solid PCM; fusion starts; fusion continues; Last solid PCM.

The PCM starts to fuse at the bottom of the storage next to the heat source. The melting region grows quickly along the two vertical aluminum walls, as the waste heat is distributed by the high thermal conductivity of the walls (Figure 6, middle left).

With time the liquid PCM region grows and natural circulation begins. It is visible during the experiments, as small bubbles move through the liquid PCM. By this natural circulation hot, liquid PCM is moved from the bottom to the

top and increases the fusion process in the upper corners of the storage (Figure 6, middle right). The solid PCM in the middle of the storage stays solid and unmoved. With all walls made of aluminum the fusion process would be different, but in this case the solid parts are kept in their position by the polycarbonate walls with low thermal conductivity.

The liquid PCM regions on the top of the storage grow due to the natural circulation of the liquid PCM until they unite in the middle and the solid PCM left in the middle of the storage (Figure 6, right). Now this remaining solid PCM is fused at last, as the overheated liquid PCM transports thermal energy to the middle. After all PCM is liquid the temperature gradient in figure 5 rises due to the continued one-phase thermal energy storage.

With the optional thermocouples inside the PCM the described effects are observed as well. Figure 7 shows the heat block temperature as a dotted, black line for a heat load of  $\dot{Q}_{low} = 50 \text{ W}$ . The solid, blue line shows the temperature of the PCM near the bottom of the heat storage. Here the gradient changes and the onset and the end of fusion are both visible at  $t = 250 \text{ s}$  and  $t = 800 \text{ s}$ . Afterward the temperature rises up to  $T = 60 \text{ }^\circ\text{C}$  where it stays constant for a while due to the natural convection. The temperature in the middle of the PCM is the dashed, green line which shows the fusion process from about  $t = 1000 \text{ s}$  to  $t = 1300 \text{ s}$ . Then the temperature rises with a steep gradient. At  $T = 80 \text{ }^\circ\text{C}$  it joins the temperature at the bottom and both rise with the same gradient, as the heat is stored sensibly in the whole storage. The air temperature above the PCM is always the lowest shown with the dash-dotted, red line.

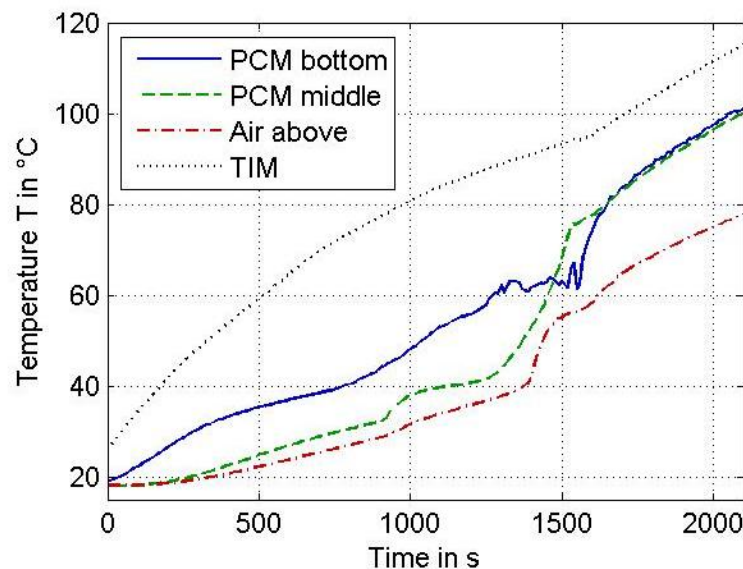


**Figure 7:** Thermal interface and PCM temperatures with U-profile for a heat load of  $\dot{Q}_{low} = 50 \text{ W}$ .

#### 4.2 Regularly structured CLHS

As described for the solid block PCM heat storage, the five surface temperatures are equal and just one temperature is plotted in figure 8. Additionally to the measured temperatures the thin straight lines show a reference temperature to simplify the assessment for mobile applications.

The thicker lines in the figure show the measured temperatures for the three different heat loads. The solid, blue line for a heat load of  $\dot{Q}_{low} = 50 \text{ W}$  demonstrates the behavior best, as the temperature rise is the slowest. Contrary to the solid block measurements the phase change process is visible with both, onset and end of fusion. The temperature rises linearly up to almost  $T = 50 \text{ }^\circ\text{C}$  as the heat block and the CLHS store the waste heat sensibly. Around  $T = 50 \text{ }^\circ\text{C}$  the fusion starts and the gradient changes as expected for latent heat storages. During the whole fusion process the temperature gradient is constant, as the waste heat is transported by the aluminum frame-structure and the PCM fuses with constant speed. Convection inside the small PCM volumes is not observed can be neglected. At  $t = 1400 \text{ s}$  the fusion is completed and all PCM turned liquid. Thus the gradient changes again, as more waste heat is stored sensibly.



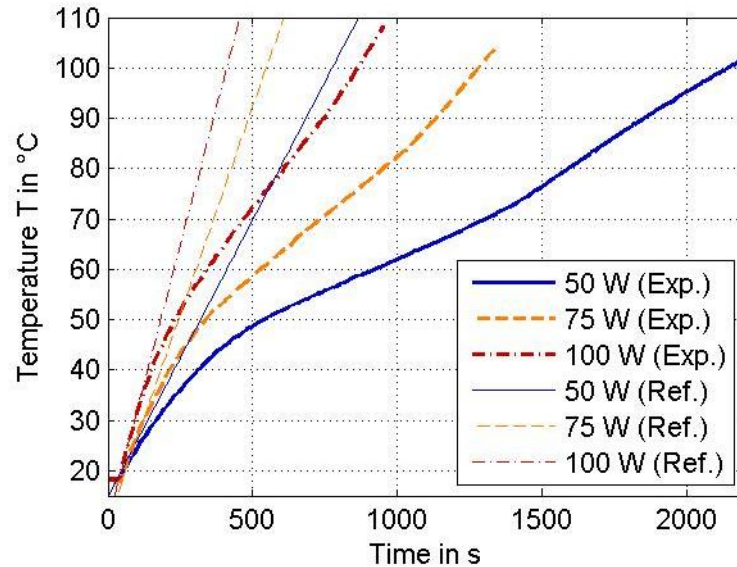


**Figure 8:** Thermal interface temperatures with frame-structure Quad for three different heat loads.

The temperature behavior for the other heat loads is qualitatively the same, however the gradient changes are not so clear any more as the temperatures rise faster and the fusion period is shorter.

For the assessment in mobile applications as e.g. civil aircraft the system weight is often a very important issue. Thus the thermal performance is compared to a solid aluminum heat storage with the same weight. The resulting reference temperature is calculated assuming ideal heat storage with a homogeneous temperature and plotted as the straight thin lines in figure 8. This shows how much longer electronic components can be used until they reach their operation temperature limit. For  $\dot{Q}_{low} = 50 \text{ W}$  and a limit temperature of  $T_{max} = 100 \text{ °C}$  the regularly structured CLHS enhances the operation time by a factor of almost 3.

The optical observation of the phase change process shows the positive impact of the frame-structure as well. Again four characteristic pictures are selected and shown in figure 9. With the frame-structure the fusion pattern changes significantly. The dark shades at the edges are part of the seal and are ignored.

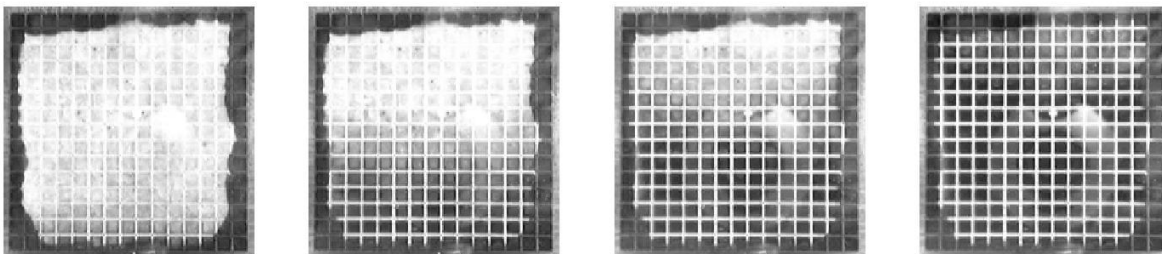


**Figure 9:** Phase change process in regularly structured CLHS prototype with quadratic frame-structure; *from left to right:* fusion starts at the bottom; phase change boundary moves upwards; fusion continues; all PCM liquid.

In the first picture the PCM at the bottom starts to fuse. Up to this time there is no difference compared to the solid block PCM heat storage (Figure 9, left).

However in the following the phase change boundary stays almost horizontally and moves upwards slowly (Figure 9, middle). This is a significant difference. The last picture shows the end of the fusion process, where all PCM is liquid and only the quadratic grid of the frame-structure is visible (Figure 9, right).

These optical observations of the phase change process confirm the often used simplification of neglecting natural convection in the modeling of PCMs, as e. g. proposed by Lamberg (2003) and Groulx and Ogoh (2009).

### 4.3 Comparison

A complete comparison of both heat storages is difficult, as the composition of the heat storage varies, i.e. the PCM and aluminum fractions are not the same. However there are large differences qualitatively. In the first place this is shown in the transient temperature behavior, which is plotted for a heat load of  $\dot{Q}_{low} = 50 \text{ W}$  in figure 10. As described above for the regularly structured CLHS the latent heat storage is clearly visible (solid, blue line), while the solid block PCM heat storage only shows the end of fusion (dashed, red line). Thus the frame-structure helps to distribute the waste heat in the storage comparably well.

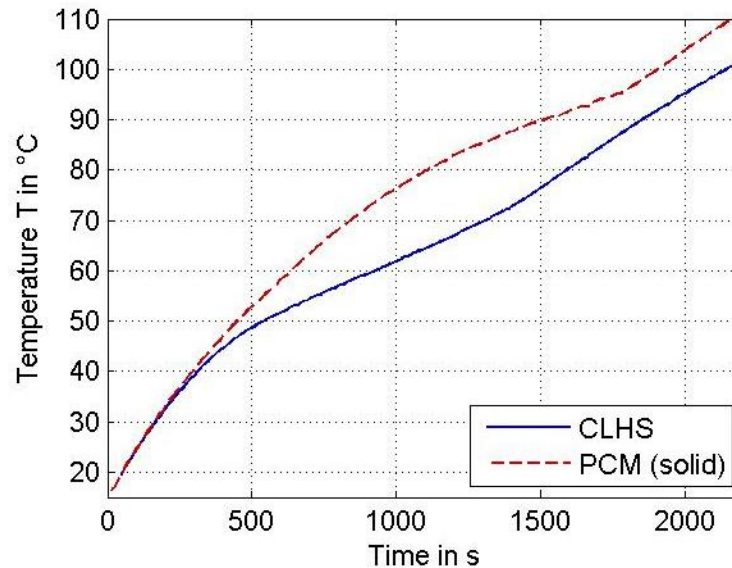


**Figure 10:** Temperatures of solid block PCM heat storage and regularly structured CLHS with quadratic frame-structure for a heat load of  $\dot{Q}_{low} = 50 \text{ W}$ .

On the other hand the optical observation of the phase change process shows significant differences. In the solid block PCM heat storage the low thermal conductivity leads to a slow phase change. This allows the liquid PCM to superheat and thus actuate natural convection, which improves the fusion process. The experiments clearly show that natural convection has to be considered in larger PCM volumes. Opposed to these results the frame-structure in the regularly structured CLHS increases the thermal conductivity and at the same time hinders natural convection. The PCM volumes are small enough, that the effect of natural convection can be neglected. However the fusion process and the advancing of the phase change boundary follow the expected pattern with the fusion starting at the heated surface at the bottom and slowly continuing upwards.

## 5. OUTLOOK

The experimental results are used to verify a simulation model presented in Lohse and Schmitz (2012). Together with the simulation model the experiments are used to develop cooling solutions for different applications. Manufacturing by SLS allows various frame-structure designs and the customization of regularly structured CLHS for special heat sources, such as electronic components like computers or actuators in aircraft systems. These high performance heat storages can be operated as back-up cooling systems in emergency cases or enable special operating conditions, e. g. longer operating times.

## 6. CONCLUSION

The work presented in this paper shows the drawback of low thermal conductivity of Phase Change Materials (PCM) and a new approach to improve the transport of thermal energy inside PCM heat storages. With a frame-

structure made of aluminum by Selective Laser Sintering (SLS), the PCM is combined to regularly structured Composite Latent Heat Storages (CLHS). These high performance heat storages can be used in aircraft cooling systems, where the system weight is crucial.

A prototype regularly structured CLHS is investigated experimentally on a test rig and the results are compared to a solid block PCM heat storage. While for the solid block PCM heat storage the phase change process is not detectable in the temperature behavior, there is a significant change of the temperature gradient for the CLHS. The phase change pattern is completely different for both prototypes as well. In the solid block PCM heat storage the transport of thermal energy is driven by natural convection due to superheated liquid PCM at the heat transfer surface. Opposed to this the natural convection is suppressed by the small structures in the CLHS and the thermal energy is transported mainly by conduction in the aluminum frame-structure.

The experiments clearly show the advantages of the combination of PCM and aluminum and the potential of manufacturing customized frame-structures designed for special cooling applications.

## NOMENCLATURE

$\alpha$	thermal diffusivity	(m <sup>2</sup> /s)	<b>Subscripts</b>	
$c$	specific heat capacity	(J/(kgK))	f	fusion
$h$	specific enthalpy	(J/kg)	high	high heat load
$k$	thermal conductivity	(W/(mK))	low	low heat load
$\dot{Q}$	heat load	(W)	max	maximum
$\rho$	density	(kg/m <sup>3</sup> )	mid	intermediate
$T$	temperature	(K, °C)		heat load
$t$	time	(s)		

### Abbreviations

CLHS	Composite Latent Heat Storage	DAQ	Data Acquisition System
PCM	Phase Change Material	SLS	Selective Laser Sintering

## REFERENCES

- COMSOL Multiphysics 2011, Materials/Coefficients Library, *COMSOL Multiphysics Documentation*, COMSOL Multiphysics 3.5a.
- Dincer, I. 2002, Thermal energy storage systems as a key technology in energy conservation, *Int. J. Energy Res*, vol 26: p. 567-588.
- Groulx, D., Ogoh, W. 2009, Solid-Liquid Phase Change Simulation Applied to a Cylindrical Latent Heat Energy Storage System, *Proc. COMSOL Users Conference, Boston*.
- Lamberg, P. 2003, Mathematical Modelling and Experimental Investigation of Melting and Solidification in a Finned Phase Change Material Storage, *Dissertation, Helsinki University of Technology (Espoo, Finland)*.
- Lohse, E., Schmitz, G. 2012, Performance Assessment of Regularly Structured Composite Latent Heat Storages for Temporary Cooling of Electronic Components, *Int. J. Refrig.* vol. 35, no 4: p. 1145-1155, Elsevier, London.
- Sasol Olefins & Surfactants GmbH, PARAFOL<sup>®</sup> Single Cut Paraffins – Technical Bulletin, Sasol Germany, <http://www.sasoltechdata.com/MarketingBrochures/PARAFOL.pdf>, May 2012.
- Srinivas, V.S.S., Ananthasuresh, G.K. 2006, Analysis and Topology Optimization of Heat Sinks with a Phase Change Material on COMSOL Multiphysics<sup>™</sup> Platform, *Proc. COMSOL Users Conference, Bangalore*.

## ACKNOWLEDGEMENT

This work is being conducted in the frame of a project funded by the Federal Ministry of Economics and Technology ([www.bmwi.de](http://www.bmwi.de)), cf. project funding reference number 20Y0803A.